

Periodic Hartree-Fock study of a weakly bonded layer structure: Brucite $\text{Mg}(\text{OH})_2$

Philippe D'Arco

*Laboratoire de Géologie de l'Ecole Normale Supérieure,
24 rue Lhomond, 75231 Paris CEDEX 05, France*

Mauro Causà and Carla Roetti

*Dipartimento di Chimica Inorganica, Chimica Fisica e Chimica dei Materiali,
Università di Torino, via Pietro Giuria 5, I-10125 Torino, Italy*

Bernard Silvi

*Laboratoire Dynamique des Interactions Moléculaires, Université Pierre et Marie Curie,
4 place Jussieu, 75230 Paris CEDEX 05, France*

(Received 14 February 1992)

The layered mineral brucite $\text{Mg}(\text{OH})_2$ is investigated theoretically using an *ab initio* all-electron linear combination of atomic orbitals Hartree-Fock (HF) approximation. At the HF level, the interlayer interaction is weak and the interlayer distance is larger than the experimental one. Bonding is discussed on the basis of density of states and charge-density maps. No hydrogen bond is characterized. *A posteriori* correction of the energy for the correlation error is performed by use of the functional approach. The three semilocal functional formulas used yield similar results. This brings in extra interlayer bonding interaction, and yields a calculated geometry in agreement with experiments. The analysis of the interlayer bondings shows that it is mainly of dispersion type, and that the used functionals account for dispersion, in particular at short interatomic distances.

I. INTRODUCTION

The most abundant natural materials on the Earth's surface, namely the clay minerals, are characterized by a layer structure and OH groups. The nature of bonds between the layers is relatively complex and depends on the chemistry of the layers. In general, it can be described by short-range Coulomb interactions and hydrogen-type bonds. These materials undergo numerous phase transformations under temperature and pressure. So there is a great need for an understanding of the energetics of such structures. However, because of their complexity we have reported our interest on a simpler structure: brucite $\text{Mg}(\text{OH})_2$, which we expect to reproduce the main features of interlayer interactions of uncharged clays. Brucite has been extensively studied experimentally because it is one of the simplest structures among hydrous minerals. The nature of interlayer bonding is largely discussed. For Bragg, Claringbull, and Taylor,¹ the layers are held together by dispersion-type forces. According to Kruger, Williams, and Jeanloz² the presence of hydrogen bonds between the layers is evidenced by the negative value of the Gruneisen parameters of the asymmetric OH stretching mode; however, Bernal and Megaw³ rejected this hypothesis on the basis of extremely large interlayer O...O distance. In any case the interlayer bonding is expected to be extremely weak as indicated by the very easy cleavage.

Brucite has been studied by Lesar and Gordon⁴ using a simple "embedded fragment" scheme, where the expressions for the kinetic, exchange, and correlation energy

are derived from the uniform electron gas theory. They optimized the geometry (at constant O-H distance: 0.982 Å) with an error of about 10% for the volume. During the preparation of the present paper an *ab initio* Hartree-Fock (HF) study of $\text{Mg}(\text{OH})_2$ was published by Sherman,⁵ where the calculations were performed with the QCPE 88 (Ref. 6) version of the CRYSTAL program used for the present study. Sherman's discussion is mainly founded on the effect of pressure on the (possible) H bonds between layers, the main conclusion being that "H bonded in brucite is very weak at zero pressure and is not enhanced with high pressure."

It is well known that Hartree-Fock (HF) calculations cannot account for dispersion energies, and therefore the corresponding stabilization contribution is missing at the self-consistent-field (SCF) level. With respect to the theory of intermolecular forces, the electrostatic, induction, and exchange penetration contributions to the interaction energy are correctly described at the HF level. Except for small corrections to these latter terms electron correlation mostly brings the dispersion contribution. This point follows from the Rayleigh-Schrödinger (RS) perturbation treatment of intermolecular forces,⁷ and also from several energy partition schemes such as Morokuma's. Extensive discussions on these topics can be found in papers by Scheiner⁸ and Bouteiller.⁹ As a consequence of these deficiencies of HF wave functions, the optimized intermolecular distances are found to be larger than experimental ones, unless basis-set incompleteness spuriously corrects this trend.

The correlation corrections are generally obtained by

the configuration-interaction technique in the case of molecules. The success of the Gordon-Kim¹⁰ method shows that density-functional approaches take into account the dispersion force although they do not seem theoretically suitable for this purpose because of their local character.

As far as we are mainly concerned in discussing the nature of the interactions responsible for the stacking of layers in brucite, it is advantageous to perform the calculations with a formalism which allows a straightforward partition of the energetic contributions. In most density-functional-theory (DFT) approaches, such a partition is hampered by the use of an exchange-correlation functional, whereas in Hartree-Fock methods the exchange contribution is exactly evaluated. As will be indicated, the correlation energy is added in a second step by means of a correlation functional of the HF density. This procedure has been shown to be theoretically justified¹¹ for the Hartree-Fock wave function. This result can be extended to the SCF wave function, provided the SCF and HF densities are close.

In the present paper we consider a certain number of points that have not been tackled in previous studies: in particular the geometry of the three-dimensional (3D) system is fully optimized; a comparison of the 3D crystal and of a single 2D layer is used for a discussion of the interlayer interactions; *a posteriori* corrections of the HF energy through correlation-only density-functional formulas are used in order to investigate the correlation contribution to the interlayer interaction. The electronic structure is described in terms of density of states, Mulliken population analysis, and charge-density maps. The evaluation of correlation contribution appears to be the key for a discussion on the nature of the interlayer forces in brucite.

II. CALCULATIONS

The calculations have been performed using CRYSTAL,⁶ an *ab initio* all-electron periodic Hartree-Fock linear-combination of atomic orbitals (LCAO) program.

A. Basis set

The "atomic orbitals" are linear combinations ("contractions") of Gaussian (*G*)-type functions (GTF). Thirteen AO's have been used for Mg and for O. The Mg basis was derived from Causà *et al.*;¹² it is an 8-5-11*G* contraction according to the notation of the Hehre and co-workers;¹³ the exponents of the two most diffuse shells, reoptimized in the bulk, are $\alpha=0.68$ and 0.28 bohr^{-2} , respectively. For oxygen we started from the 8-411*G* contraction used by Dovesi *et al.*¹⁴ in the study of Li_2O , Na_2O , and K_2O ; the exponents of the two most diffuse shells have been reoptimized ($\alpha_{3sp}=0.50$ and $\alpha_{4sp}=0.20 \text{ bohr}^{-2}$). For H we use the Pople 21*G* (Ref. 13) standard basis set. We shall indicate this basis set as *standard* (SB). However, to test the validity of the presented results, numerous calculations have been performed with this basis set extended by addition of *p*- and *d*-polarization functions on H ($\alpha=1.1 \text{ bohr}^{-2}$) and O

($\alpha=0.8 \text{ bohr}^{-2}$), respectively. The corresponding results will be indicated as SB_{+p}, SB_{+d}, SB_{+pd}.

The reciprocal space integration is performed by using a commensurate net, the meshes of which are determined by the shrinking factors *S*. *S*=6 (corresponding to 6 and 34 *k* points for the slab and bulk, respectively) has been used for the present calculations; when *S*=12 is used the energy change is less than 10^{-6} a.u., which is the SCF convergence threshold.

B. Estimation of the correlation energy

The HF results are known to be affected by the so-called "correlation error"; for typical covalent systems (III-IV semiconductors), the error is of the order of -30-50% for the binding energy (BE), 1% for the lattice parameters, and 7% for the force constants.¹⁵ The simplest way for correcting this error consists in using density-functional-like correlation-only formulas. The correction consists in integrating a function of the HF density (obtained at a given geometry) over the unit cell. Such a procedure can be seen as a variant of the DFT-based computational schemes, the differences being (a) the "exact" Hartree-Fock exchange is used, instead of the approximate one; (b) the DF-based correlation correction is applied *a posteriori*, so that only the energy is corrected but not the wave function. Three different functionals, proposed by Colle and Salvetti¹⁶ in 1975 (CS), Perdew¹⁷ in 1986 (P86), and Perdew¹⁸ in 1991 (P91) have been considered for comparison. It is to be noticed that the three correlation-only functionals are "nonlocal," in the sense that they contain terms depending not only on the charge density at a given point, but also on its gradient. The most recent functional (P91) is parameter-free, whereas the others contain a "universal" parameter whose value was obtained by requiring that the functional reproduce the exact correlation energy of the He (CS) and Ne (P86) atoms. In this respect they are expected to perform better than the older local functionals, such as those proposed by Wigner,¹⁹ Hedin and Lundquist,²⁰ and Ceperley and Alder.²¹ In their systematic study of structural properties of the III-IV semiconductors, Causà, Dovesi, and Roetti¹⁵ found that the mean error on the BE is reduced to 3% by use of the P86 functional.

C. Optimization

The structure of brucite, as resulting from neutron diffraction experiments,^{24,25} is shown in Fig. 1; the space group is $D_{3d}^3(P3m1)$; brucite has a layered structure with the OH groups orthogonal to the hexagonal basal plane. The structure is usually described by four parameters: *a*, *c*, and the two fractionary coordinates of O and H (z_{O} and z_{H} in the following). It is, however, more convenient to refer to crystallographic internal coordinates, in particular in the geometry optimization. In the present case we refer to the Mg-O and O-H bond lengths and the H · · · H (interlayer) and O-O (within the layer) distances (see Fig. 1). They are related to the previous variables by the following relations:

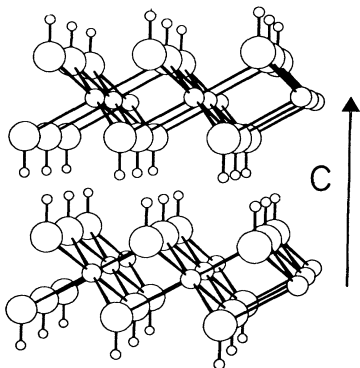


FIG. 1. Perspective view of the brucite crystal, a fragment of two layers is reported. Large, medium, and small circles represent O, Mg, and H atoms, respectively.

$$\text{Mg-O} = \left[\frac{a^2}{3} + c^2 z_O^2 \right]^{1/2},$$

$$\text{O-H} = c(z_H - z_O),$$

$$\text{O-O} = \left[\frac{a^2}{3} + 4c^2 z_O^2 \right]^{1/2},$$

$$\text{H} \cdots \text{H} = \left[\frac{a^2}{3} + c^2(1 - 2z_H)^2 \right]^{1/2}.$$

The two available experimental geometries (both obtained by using neutron diffraction) are reported in Table I. One of the crucial points discussed in the literature is the nature of the interlayer interaction, which has been attributed to hydrogen bond by some authors. It is to be noticed that the O-H \cdots H group is not linear ($\widehat{\text{OHO}} = 140^\circ$) unlike the classical H bond,²² and that the O \cdots O distance (3.2 Å) is larger, and the O-H distance is shorter than usual in hydrogen bonded structures,²² such as KDP.²³

The calculated equilibrium structure was obtained by minimizing the total (internal) energy point by point. The crystallographic coordinates were optimized one by one, and the search was repeated until a self-consistent set of one-dimensional minima was found. The optimization was performed using the "standard basis" (SB, see above).

III. RESULTS

A. HF bulk structure

The calculated and experimental bulk structures are reported in Table I. The experimental structures^{24,25} obtained at room temperature are not corrected for thermal effects. The table shows a reasonable agreement between the calculated and experimental data. However, one should distinguish between intra- and interlayer parameters.

Within the layer, the percentage errors for the Mg-O, O-O distances are less than 1%, and slightly more on O-H (<3%). The calculated O-H distance agrees with the one reported by Sherman.⁵ However, some more discussion is needed about the experimental O-H distance. The two experimental structures are very similar for all parameters but the O-H bond length. There are indications that the distance reported by Zigan and Rothbauer²⁴ is too long. First, the mean O-H bond length resulting from NMR experiments²⁶ is 0.98 Å. It is well known²⁷ that the NMR distance is longer than the neutron one, which is calculated with respect to the mean position of the atoms. Taking into account thermal motion effects²⁸ one obtains a mean distance of 1.03 and 0.97 Å from the Zigan-Rothbauer²⁴ and Catti-Ferraris-Hull²⁵ data, respectively. Second, the OH neutron distance in portlandite [Ca(OH)₂, same structure as brucite] is 0.94 Å (0.98 Å after correction for thermal motion),²⁸ quite close to the result of Catti, Ferraris, and Hull.

The discrepancy between present calculation and experiment for the parameters describing the interlayer distance (*c* axis and H \cdots H distance) is somewhat larger than for the other parameters. The *c* lattice parameter is overestimated by about 12%. This discrepancy is slightly larger than the one calculated by Lesar and Gordon.⁴

It is to be noticed that the volume calculated in this study (45.9 Å³) is larger by 12% than the one reported by Sherman.⁵ This difference is surprising because the same method and comparable basis sets have been used. However, apparently Sherman did not optimize independently the *c* and *a* lattice parameters but the *c/a* ratio at constant volume. The cell parameters are not reported.

In Fig. 2, the HF energy is reported versus the *c* axis. The curve presents a shallow minimum of about 0.0017 hartree with respect to the very large *c* limit. The HF solution corresponds to under bonded layers with respect to the experimental structure. In order to check the weakness of the interlayer interactions, single-layer calculations have been performed. The optimized slab

TABLE I. Calculated and experimental (at room temperature) structural parameters of brucite. All values in angstroms.

	<i>a</i>	<i>c</i>	Mg-O	O-O	O-H	H-H
This work	3.146	5.354	2.103	2.787	0.953	2.250
Expt. ^a	3.142	4.766	2.102	2.787	0.995	1.932
Expt. ^b	3.148	4.769	2.096	2.767	0.927	1.997

^aReference 24.

^bReference 25.

TABLE II. Influence of the basis set on the total energy of the bulk (3D) and of the corresponding single layer (2D). Symbols for the different basis sets are defined in the text. Δ is the difference between the bulk and the slab energy. All quantities refer to a single $\text{Mg}(\text{OH})_2$ unit and are in hartrees.

	SB	SB_{+p}	SB_{+d}	SB_{+p+d}
Bulk	-350.7278	-350.7476	-350.7396	-350.7503
Slab	-350.7262	-350.7457	-350.7374	-350.7484
Δ	-0.0016	-0.0019	-0.0022	-0.0019

geometry matches exactly the one of the layer in the bulk, in particular the O-H distance in the bulk is not increased in contrast with SCF calculations on true hydrogen bonded systems.²⁹ The energy of the optimized slab is reported in Fig. 2; as one can see, the energy difference with a 3D crystal characterized by a large c axis (6.8 Å) is extremely small (3×10^{-5} hartree). As will be discussed later, the electronic properties of the bulk and the slab are very similar.

At the SCF level, the optimized lattice parameter c value depends upon the basis set used. Computational experience on systems involving OH bonds, such as ice VIII, indicates that the maximum relative difference between polarized and unpolarized basis set results in less than 2% on bond lengths. Moreover, as indicated later on, a few energy points have been calculated with polarized basis sets showing an almost constant downward energy shift independently of the geometry. Accordingly, 0.1 Å has to be considered as a reasonable upper bound to the basis-set-dependent uncertainty on the lattice parameter.

As the energy difference between the bulk and the slab is extremely small, it is necessary to check the effect of larger basis-set upon this difference. However, due to the computer cost, the bulk and slab structures have not been reoptimized using the SB_{+p} , SB_{+d} , and SB_{+pd} basis sets. The large basis-set energies have been calculated at the SB optimized geometry. As indicated by the values quoted in Table II, the energy difference is almost constant as

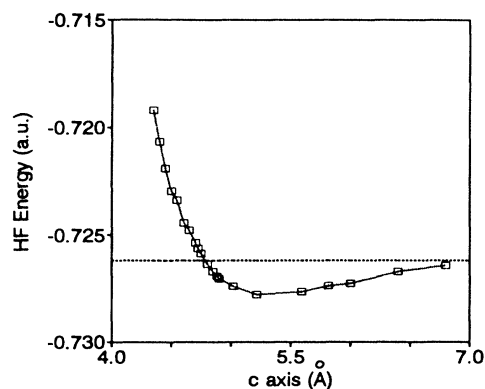


FIG. 2. Hartree-Fock energy of brucite vs the c axis (Å). The horizontal dashed line indicates the single-layer slab energy. The energies have been shifted by 350.000. Energy in hartrees.

a function of the basis set. This suggests that the inter-layer bonding should not be modified by the use of even larger basis sets at the HF level.

The influence of the basis set upon the geometry parameters has been explored only for the OH distance in 2D single-layer slabs. The use of polarization functions yields a shortening of the O-H distance from 0.95 to 0.94 Å, as is usually observed. Due to the very small inter-layer interactions, these results are probably valid also for the 3D structure. The agreement with the O-H distance reported by Catti, Ferraris, and Hull is enhanced.

As previously indicated, the O-H \cdots O configuration is not linear, unlike in the classical H bonded compound. In order to check the possibility of a linear static O-H \cdots O geometry, the OH groups have been tilted relative to the c axis. However, the calculations were performed with smaller basis sets: STO-3G (Slater-type orbital fitted to contractions of three Gaussian functions) and 3-21G for Mg and O, respectively, because of the breakdown of the symmetry. The investigated configurations with linear O-H \cdots O are found less stable than the opti-

TABLE III. Energy data for brucite (left), for the Mg, O, and H atoms (right). E , BE, and CE are the total Hartree-Fock, binding energy, and the correlation energies, respectively, CS, P86, and P91 refer to the three functionals used for the evaluation of CE. The four values in the left part refer to the different basis set (see text). The experimental (expt.) value of the BE has been calculated from thermochemical data (Ref. 30). (Energy in hartrees.)

	Brucite $\text{Mg}(\text{OH})_2$				Mg	O	H
	SB	SB_{+p}	SB_{+d}	SB_{+pd}			
E (HF)	-350.7278	-350.7476	-350.7396	-350.7503	-199.6044	-74.8013	-0.4962
BE (HF)	0.528	0.548	0.540	0.551			
CE (CS)					-0.4513	-0.2588	0.0000
BE (HF+CS)	0.682	0.702	0.694	0.705			
CE (P86)					-0.4648	-0.2614	-0.0030
BE (HF+P86)	0.716	0.736	0.728	0.739			
CE (P91)					-0.4478	-0.2552	-0.0070
BE (HF+P91)	0.697	0.717	0.709	0.720			
BE (expt.)	0.756						

mized structure with the OH groups parallel to the c axis.

The binding energies and all the relevant data are reported in Table III. The atomic energies of Mg and O have been obtained by supplying two more sp shells to Mg and reoptimizing the exponent of the external sp shell of O ($\alpha=0.208$ bohr $^{-2}$). The HF BE corresponding to the SB represents about 70% of the value estimated from thermochemical data.³⁰ Using the SB $_{+pd}$ basis sets, 73% of the experimental BE is recovered. As will be discussed later, most of the missing BE is due to correlation effects.

B. Analysis of the electronic structure

1. Density of states

The calculated total and projected densities of states (DOS) of the bulk and slab are represented in Figs. 3(a)

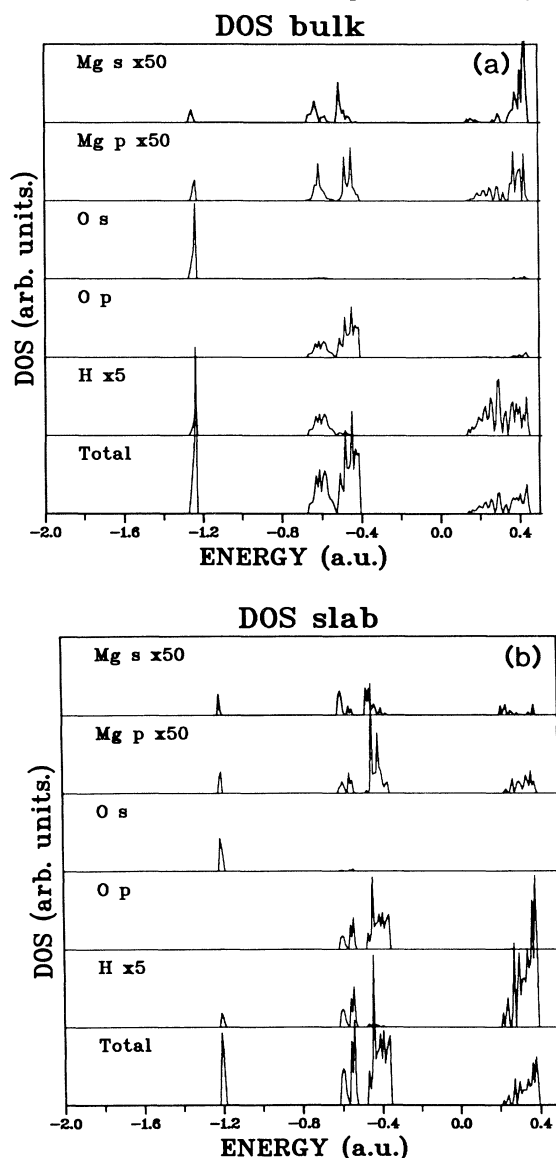


FIG. 3. Total and projected DOS of brucite. (a) 3D crystal; (b) single-layer slab. $\times 50$ and $\times 5$ indicate that contributions of the Mg and H states have been multiplied by 50 and 5, respectively.

and 3(b), respectively. They are very similar, confirming the weakness of the interlayer interactions. However, a few minor differences can be detected: the small gap in the slab at about -0.5 hartree, and the different contribution of H to the bands centered at -0.5 and -1.2 hartree, for example. The DOS show the typical features of ionic systems with large gaps between bands. The valence bands are split in two parts. The highest one, between -0.7 and -0.4 hartree, corresponds mainly to O_{2p} states with a strong contribution from the hydrogen. The lowest one, below -1.20 hartree, is mainly due to the O_{2s} states again with a non-negligible hydrogen contribution. This mixed O-H contribution to the valence bands indicates the strong covalent character of the OH bond. The Mg contribution is extremely small; the MgO bond population is very small ($+0.01e$), and for the B1 phase of MgO a small negative value ($-0.01e$) was found.¹² The Mulliken net charge of Mg is $+1.86$ compared to $+1.99$ in MgO-B1. The O and H net charges are -1.325 and $+0.396$, respectively (with the SB), and the OH bond population is 0.222. This confirms that the OH bond has a strong covalent character. These results agree with the interpretation of x-ray fluorescence spectra proposed by Haycock *et al.*³¹

The calculated total DOS can be compared to the x-ray photoelectron spectrum. However, since the zero of the one-electron energy level is arbitrarily defined, and the experimental zero energy is fixed with some arbitrariness, the ends of the higher-energy limit of the uppermost calculated and experimental peaks have been superposed. As shown in Fig. 4, there is a reasonable qualitative agreement between the calculated and the experimental spectra, although the calculated lower peak is shifted toward negative values with respect to the experimental one. The overestimation of band gaps is a well-known feature of the HF method³² that has been well illustrated, among others, by Nada *et al.*³³

2. Deformation of electron density

The total and difference (bulk minus atomic superposition) charge-density maps in the (110) plane are shown in Figs. 5(a) and 5(b). The Mg atoms are at the corners of the figures. It is clearly shown that the charge transfers towards the oxygen centers, and the covalent OH bond. In order to explore the difference between the bulk and

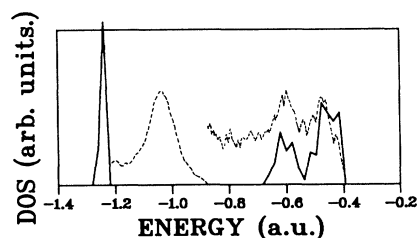


FIG. 4. Comparison between calculated total DOS (continuous line) of brucite and x-ray photoelectron spectrum (Ref. 31) (dashed line). The experimental high-energy peak was recorded with a full scale three times larger than the one used for the low-energy ones.

the single-layer slab charge distributions, we performed a difference map between the two systems [Fig. 5(c)]. No gain of electrons is observed along the $\text{H} \cdots \text{O}$ directions. In the bulk the hydrogen centers are slightly depleted relatively to the slab, with a Mulliken net charge of $+0.396$ instead of $+0.346$. This corresponds to an electron transfer from the hydrogen to the nearest oxygen in the layer, and not to a transfer towards the oxygen in the next layer. The net charge of the oxygen atoms decreases from -1.280 in the slab to -1.325 in the bulk. As can be deduced from the map, the net charge on Mg is almost constant.

The $\text{O} \cdots \text{H}$ bond population is extremely small: $0.004e$. This value has to be compared to $0.04e$ and $0.03e$ obtained for H bonds in the bulk urea using basis sets of quality comparable to that used in this work.³⁴

IV. DISCUSSION

At the HF level, the calculations partly fail to produce the observed structure. The layers are under bonded, and the c axis is too long by about 12%. No hydrogen bond has been characterized, although hydrogen bonding is accounted for at this level.³⁴ We recall that it is widely believed that the dominant contribution to hydrogen bonding is the classical electrostatic term³⁵⁻³⁷ which is almost exactly taken into account in the method used. The attempt to produce distorted structures with linear $\text{O}-\text{H} \cdots \text{O}$ bonds fails. In addition, 30% of the BE is not recovered. These results must be considered as "genuine" in the sense that basis-set effects and numerical approximations are expected to have negligible influence on them.

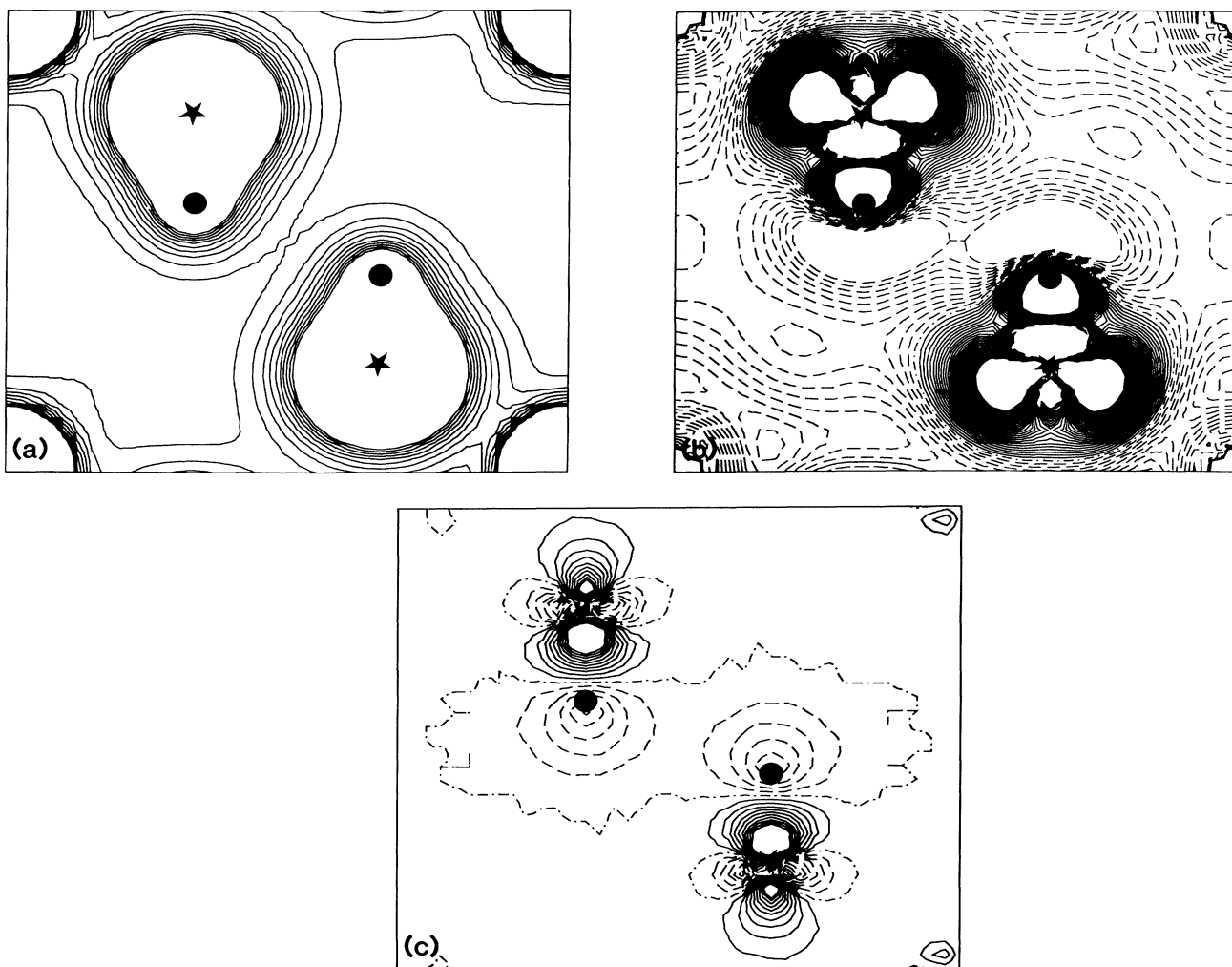


FIG. 5. Total (a) and difference (b,c) charge-density maps of brucite in the (110) plane through four Mg atoms (at the corners). (b) shows the difference between the bulk charge density and the charge density resulting from the superposition of atomic charges; (c) displays the difference between bulk and slab densities. Continuous, dot-dashed, and dashed lines refer to positive, null, and negative values. The interline spacing is 0.01 (a) and 0.001 (b,c) e/bohr^3 . Stars and dots represent O and H atoms, respectively.

As previously indicated, the HF calculations are biased by the so-called "correlation error." At the present state of the LCAO periodic *ab initio* techniques, calculations of correlated wave functions are not yet possible. So we apply *a posteriori* density-functional-like correlation formulas to the HF density to estimate the correlation error (CE). The CE has been estimated as a function of the c axis using the three functionals mentioned previously. In Fig. 6, the total energy (HF+CE) is represented versus the c axis. Despite some numerical noise, the minimum is clearly shifted toward smaller c values with respect to the HF minimum. The minima are approximately at 4.76, 4.64, and 4.72 Å for CS,¹⁶ P86,¹⁷ and P91 (Ref. 18) functionals, respectively. The c lattice parameter is now in excellent agreement with the experimental values (4.77 Å).

The BE calculated from the total energies corrected for the correlation error are quoted in Table III. They represent at least 90% of the expected value. Part of the residual error (probably of the order of 0.03 hartree) is due to the basis-set incompleteness, as clearly shown by Tables II and III. We must indicate that the CE is almost basis set independent: the variations are of the order of the numerical integration accuracy (10^{-4} hartree).

It is to be noticed that the three correlation formulas give quite similar results, in spite of the different functional form. However, such correction is incomplete because it does not involve the intralayer geometrical parameters. Partial optimization of the crystal structure within this *a posteriori* scheme yields a reduction of the a parameter of about 0.09 Å (from 3.146 to 3.055 Å).

A posteriori corrections for the CE yield structures and BE in close agreement with experimental data, thanks to the correlation correction.

The correlation contribution can be partitioned into two kinds of contribution: on the one hand is an intralayer correlation correction, and on the other hand is the interlayer one which is expected to account for most

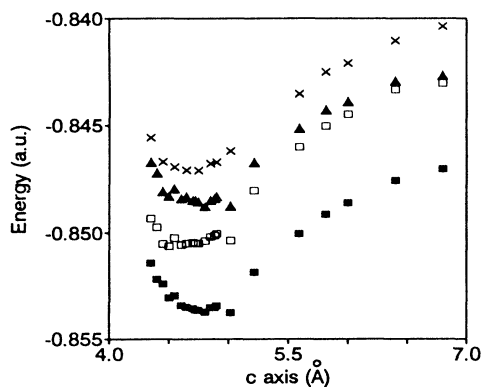


FIG. 6. Total energy vs the c axis (Å). Solid squares, open squares, and solid triangles correspond to total energies (HF+CE) obtained for CS, P86, and P91 functionals, respectively. Crosses represent HF+dispersion energy. Energy shifts of 351.000, 351.060, 351.022, and 350.224 have been applied to total energies obtained for CS, P86, P91, and dispersion energy, respectively. Energy in hartrees.

of the dispersion energy. Within this partition scheme, the interlayer contribution, which can be estimated from calculations performed on a single-layer slab or on bulk crystal with large c lattice parameter, represents less than 0.7% of the total correlation energy correction. The interlayer correction, ≈ 0.007 hartree, at the equilibrium geometry ($c \approx 4.75$ Å) is four times larger than the HF stabilization energy of the bulk relative to the single-layer slab.

It is interesting to compare these results with the thorough analysis of the intermolecular forces contribution of Hess *et al.*³⁸ performed on the water dimer, which is a typical case of a hydrogen bonded complex. For this dimer, the different contributions to the intermolecular binding accounted for at the SCF level represent 72% of the interaction energy. The remaining contribution contains an attractive part which is mostly of dispersive nature and a repulsive one involving second-order exchange corrections. Moreover for this system, the SCF molecular separation is shorter than the experimental one. Though it is not clear how density functionals describe dispersion interactions, it is obvious from our results on brucite that, at least in this case, such a method works successfully. Numerical evidence of the ability of density functionals to account for dispersion can be found in calculations on solid argon,³⁹ and helium⁴⁰ in which all the attractive energy results from dispersion effects.

As an alternative to purely *ab initio* techniques, the dispersion energy can be evaluated from dispersion coefficients by using a simple r^{-6} formula. Among the dispersion effects, a nonminor role should be played by the interactions involving O and H. We used the consistent set of dispersion coefficients derived by Spackman⁴¹ to estimate the dispersion energy (DE) of the bulk and single-layer slab. In Fig. 6, the total energy (HF+DE) is reported versus the c axis. The corresponding curve compares quite well to those derived from the correlation correction; its minimum, located at about 4.68 Å, is in agreement with the minimum of the correlated curves.

The interlayer DE (defined as a difference between DE of the bulk and DE of single-layer slab) is compared to

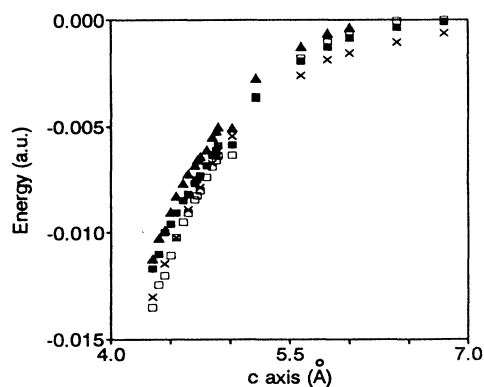


FIG. 7. Interlayer interaction correlation and dispersive energy. Symbols as in Fig. 6. Energy in hartrees.

the equivalent quantities derived from the estimates of the CE in Fig. 7; the agreement is quite surprising. However, at short distances ($c < 5.2$ Å) the various sets of values behave similarly, whereas at larger distances the interlayer CE vanishes more rapidly than the interlayer DE. This is due to the breakdown of the "semilocal" approximation of the functionals when the atomic overlaps go to zero.

In a comparable study of MgCl_2 , which is isostructural to brucite, Harrison and Saunders⁴² found that the layers are unbonded at the HF level. The agreement with the experimental data is achieved by considering the dispersion forces between nearest chlorine anions.

From this discussion, it appears that the CE may involve dispersion effects. In the present case, the $\text{H} \cdots \text{H}$,

$\text{O} \cdots \text{O}$, and $\text{H} \cdots \text{O}$ dipolar interactions seem responsible for this contribution. This supports the conclusion by Busing and Levy²⁸ that van der Waals forces stabilize the layer structure.

ACKNOWLEDGMENTS

The calculations have been performed on the VP200 of CIRCE (CNRS) which is gratefully acknowledged. This work has been financially supported by CNRS Grant No. DBT 89ATP668AP89. Laboratoire de Géologie de l'École Normale Supérieure is URA1316 of the CNRS. Laboratoire Dynamique des Interactions Moléculaires is ER271 of the CNRS.

- ¹L. Bragg, G. F. Claringbull, and W. H. Taylor (unpublished).
- ²M. B. Kruger, Q. Williams, and R. Jeanloz, *J. Chem. Phys.* **91**, 5910 (1989).
- ³J. D. Bernal and H. D. Megaw, *Proc. R. Soc. London, Ser. A* **151**, 384 (1935).
- ⁴R. Lesar and R. G. Gordon, *Phys. Rev. B* **25**, 7221 (1982).
- ⁵D. M. Sherman, *Am. Mineral.* **76**, 1769 (1991).
- ⁶R. Dovesi, C. Pisani, C. Roetti, M. Causà, and V. R. Saunders, QCPE program No. 577, Quantum Chemistry Program Exchange, Indiana University, Bloomington, Indiana, 1989.
- ⁷P. Claverie, in *Intermolecular Interactions: From Diatomics to Biopolymers*, edited by B. Pullman (Wiley, New York, 1978), p. 69.
- ⁸S. Scheiner, in *Theoretical Models of Chemical Bonding*, edited by Z. B. Maksic (Springer, Berlin, in press).
- ⁹Y. Bouteiller, in *Trends in Chemical Physics*, edited by J. Menon (CSRI, Trivandrom, 1991).
- ¹⁰R. G. Gordon and Y. S. Kim, *J. Chem. Phys.* **56**, 3122 (1972); Y. S. Kim and R. G. Gordon, *ibid.* **60**, 1842 (1974).
- ¹¹M. Levy, in *Density Matrices and Density Functionals*, edited by R. Erdahl and V. H. S. Smith, Jr. (Reidel, Dordrecht, 1987).
- ¹²M. Causà, R. Dovesi, C. Pisani, and C. Roetti, *Phys. Rev. B* **33**, 1308 (1986).
- ¹³J. S. Binkley, J. A. Pople, and R. F. Hehre, *J. Am. Chem. Soc.* **102**, 939 (1980).
- ¹⁴R. Dovesi, C. Roetti, C. Freyria-Fava, and M. Prencipe, *Chem. Phys.* **156**, 11 (1991).
- ¹⁵M. Causà, R. Dovesi, and C. Roetti, *Phys. Rev. B* **43**, 11937 (1991).
- ¹⁶R. Colle and O. Salvetti, *Theor. Chim.* **37**, 329 (1975); *J. Chem. Phys.* **79**, 1404 (1983).
- ¹⁷J. P. Perdew, *Phys. Rev. B* **33**, 882 (1975); **34**, 7406 (E) (1986).
- ¹⁸J. P. Perdew, *Electronic Structure of Solids 91*, edited by P. Ziesche and H. Eschrig (Akademie Verlag, Berlin, 1991), p. 11; J. P. Perdew and Y. Wang (unpublished); J. P. Perdew, J. A. Chevary, S. H. Vosko, K. A. Jackson, M. R. Pederson, D. J. Singh, and C. Fiolhais, *Phys. Rev. B* **46**, 6671 (1992).
- ¹⁹E. Wigner, *Phys. Rev.* **46**, 1002 (1934).
- ²⁰L. Hedin and B. I. Lundqvist, *J. Phys. C* **4**, 2064 (1971).
- ²¹D. M. Ceperley and B. J. Alder, *Phys. Rev. Lett.* **45**, 566 (1980).
- ²²P. Hobza and R. Zahradnik, *Chem. Rev.* **88**, 871 (1988).
- ²³Z. Tun, R. J. Welmes, W. F. Kuhs, and R. F. D. Stansfield, *J. Phys. C* **21**, 245 (1988).
- ²⁴F. Zigan and R. Rothbauer, *Neus. Jahr. Mineralg. Monatshefte* **4-5**, 137 (1967).
- ²⁵M. Catti, G. Ferraris, and S. Hull (unpublished).
- ²⁶D. D. Elleman and D. Williams, *J. Chem. Phys.* **25**, 742 (1956).
- ²⁷B. T. M. Willis and A. W. Pryor, *Thermal Vibrations in Crystallography* (Cambridge University Press, Cambridge, 1975), p. 280.
- ²⁸W. R. Busing and H. A. Levy, *J. Chem. Phys.* **26**, 563 (1957).
- ²⁹B. O. Ross, W. P. Kraemer, and G. H. F. Dierksen, *Theor. Chim. Acta* **52**, 77 (1976).
- ³⁰*Handbook of Chemistry and Physics*, 67th ed., edited by R. C. Weast (CRC, Boca Raton, FL, 1987).
- ³¹D. E. Haycock, M. Kasrai, C. J. Nicholls, and D. S. Urch, *J. Chem. Soc. Dalton Trans.* **12**, 1791 (1978).
- ³²C. Pisani, R. Dovesi, and C. Roetti, in *Hartree-Fock Ab Initio Treatment of Crystalline Systems* (Springer-Verlag, Berlin, 1988).
- ³³R. Nada, C. R. A. Catlow, R. Dovesi, and C. Roetti, *Phys. Chem. Minerals* **17**, 353 (1990).
- ³⁴R. Dovesi, M. Causà, R. Orlando, C. Roetti, and V. R. Saunders, *J. Chem. Phys.* **92**, 7402 (1990).
- ³⁵R. Rein, in *Intermolecular Interactions: From Diatomics to Biopolymers*, edited by B. Pullman (Wiley, New York, 1978), p. 307.
- ³⁶P. Schuster, in *Intermolecular Interactions: From Diatomics to Biopolymers*, edited by B. Pullman (Wiley, New York, 1978), p. 363.
- ³⁷K. Morokuma and K. Kitaura, in *Molecular Interactions*, edited by H. Ratajczak and W. J. Orville-Thomas (Wiley, New York, 1980), p. 21.
- ³⁸O. Hess, M. Caffarel, C. Huiszoo, and P. Claverie, *J. Chem. Phys.* **92**, 6049 (1990).
- ³⁹R. Lesar, *J. Phys. Chem.* **88**, 4272 (1984).
- ⁴⁰R. Colle, F. Bassani, and T. O. Woodruff, *Nuovo Cimento* **9**, 1145 (1987).
- ⁴¹M. S. Spackman, *J. Chem. Phys.* **85**, 6579 (1986), lines 2 and 6 of Table IV.
- ⁴²N. M. Harrison and V. R. Saunders, *J. Phys. Condens. Matter* **4**, 3873 (1992).